



Target-based drug discovery, ADMET profiling and bioactivity studies of antibiotics as potential inhibitors of SARS-CoV-2 main protease (M^{Pro})

Misbaudeen Abdul-Hammed¹ · Ibrahim Olaide Adedotun¹ · Victoria Adeola Falade¹ · Adewusi John Adepoju¹ · Sabitu Babatunde Olasupo³ · Modinat Wuraola Akinboade²

Received: 23 March 2021 / Accepted: 15 June 2021 / Published online: 1 July 2021
© Indian Virological Society 2021

Abstract A recent outbreak of a new strain of Coronavirus (SARS-CoV-2) has become a global health burden, which has resulted in deaths. No proven drug has been found to effectively cure this fast-spreading infection, hence the need to explore old drugs with the known profile in tackling this pandemic. A computer-aided drug design approach involving virtual screening was used to obtain the binding scores and inhibiting efficiencies of previously known antibiotics against SARS-CoV-2 main protease (M^{Pro}). The drug-likeness analysis of the repurposed drugs were done using the Molinspiration chemoinformatics tool, while the Absorption, Distribution, Metabolism, Excretion, and Toxicity (ADMET) analysis was carried out using ADMET SAR-2 webserver. Other analyses performed include bioactivities of the repurposed drug as a probable anti-SARS-CoV-2 agent and oral bioavailability analyses among others. The results were compared with those of drugs currently involved in clinical trials in the ongoing pandemic. Although antibiotics have been speculated to be of no use in the treatment of viral infections, literature has emerged lately to reveal the antiviral potential and immune-boosting ability of antibiotics. This study identified Tarivid and Ciprofloxacin with binding affinities of – 8.3 kcal/mol and – 8.1 kcal/mol, respectively as significant inhibitors of SARS-CoV-2 (M^{Pro}) with better

pharmacokinetics, drug-likeness and oral bioavailability, bioactivity properties, ADMET properties and inhibitory strength compared to Remdesivir (– 7.6 kcal/mol) and Azithromycin (– 6.3 kcal/mol). These observations will provide insight for further research (clinical trial) in the cure and management of COVID-19.

Keywords COVID-19 · SARS-CoV-2 main protease (M^{Pro}) · Molecular docking · Antibiotics · ADMET profiling

Introduction

The outbreak of a respiratory tract infection identified in a cluster of pneumonia patients in Wuhan China has become a global health challenge that cut across all continents of the world [10]. The previously unknown causative virus was later identified as novel CoV-19 by the world health organization [11] and since it has symptoms close to Severe Acute Respiratory Syndrome Coronavirus, hence the name SARS-CoV-2. According to John Hopkins Coronavirus Resource Centre (<https://coronavirus.jhu.edu/map.html>), the number of confirmed and death cases are increasing globally on daily basis, with more than 174,433,374 confirmed and 3,758,217 death cases reported so far as at the time of this report. The disease was referred to as pandemic rather than epidemic because of the rate and speed of transmission. These figures revealed that SARS-CoV-2 is a life-threatening disease that has become a major health concern worldwide. Despite efforts from government officials and private establishments to curtail the spread and effects of this virus, our world is yet to be free, the figures continue to rise as the world is currently experiencing the second wave of the pandemic with no

✉ Misbaudeen Abdul-Hammed
mabdul-hammed@lautech.edu.ng

¹ Department of Pure and Applied Chemistry, Ladoke Akintola University of Technology, P.M.B. 4000, Ogbomoso, Nigeria

² Department of Biochemistry, Ladoke Akintola University of Technology, P.M.B. 4000, Ogbomoso, Nigeria

³ National Agency for Food and Drug Administration and Control (NAFDAC), Abuja, Nigeria

permanent cure so far. Millions of lives have been lost coupled with numerous social and economic crises, thus putting researchers on the red alert and necessitate continuous research through repurposing old drugs, developing vaccines, identifying novel lead compounds from plants, and synthesizing new drug molecules. Symptoms include cough, fever, short breathing, chest pain, sore throat, and lower respiratory tract symptoms [13].

Over the years, antibiotics have been a strong resort in a bid to cure the infection pathway and have tremendously saved several millions of lives [9]. Administration of these antibiotics recorded great success both in the developed and developing world due to low morbidity and mortality rate [2]. Despite its efficacy as an antimicrobial agent, antibiotics have been speculated to either be of no use or inappropriate in the treatment of viral infections including respiratory tract infections, except for pneumonia which regardless of its etiology is still treated with antibiotics [7, 54]. Hence its place in the treatment/management of SARS-CoV-2 (COVID-19) is questionable.

More recently, literature has emerged that offers contradictory findings of the inappropriate use of antibiotics in viral infections; In 2016, an experiment undertaken by Karst pointed out that there exists a relationship between commensal bacteria and viruses, and that this relationship enhances and facilitates the binding of the virus to the host cell, he, however, revealed that the depletion of commensal bacterial with antibiotics reduced viral load and replication in the host cell [29]. Also, Gopinath and his team reported that topical administration of aminoglycoside antibiotics reduced viral replication and also increased host resistance to viral infections like influenza A, Zika virus, and herpes virus without depletion of commensal bacteria [21]. Similarly, topical administration of neomycin (a nontoxic vagina aminoglycoside antibiotics) on immunized rats induced with the herpes virus, enhance the immune response of the host and hence conferred protection against the virus, noting that there was no protection in the absence of immunization vaccine [22], this research complement the findings of Miller, that Childhood bacillus Calmette-Guerin (BCG) vaccination reduced the number of reported cases, morbidity, and mortality in the ongoing COVID-19 pandemic [42]. In another research, azithromycin, a macrolide antibiotic was found to inhibit replication of the Zika virus [46] as well as the reduction in viral load and inactivation of endocytic activity of newly budded progeny in the human influenza virus [57]. Collectively, these studies highlight the unexpected antiviral potential of antibiotics.

As the struggle in finding a lasting solution to this world threat (COVID-19) continues, many commercial drugs (antibiotics & antiviral) and vaccines have been used and subjected to randomized clinical trials. A lot has been done on vaccine development using different

immunoinformatics framework. The use of SARS-CoV-2 spike glycoprotein for the development of a robust and efficient vaccine against this deadly viral infection has been reported [31], while credible vaccine mechanism that can trigger the immune response to apprehend this deadly virus has also been identified [34]. Other notable research in the development of vaccines against unmet medical needs includes the development of effective cytotoxic T-lymphocyte epitope to engender a prudent response against carcinogenic melanoma-associated antigen-A11, as well as formulation and optimization of multi-epitope subunit vaccine using computational techniques to arrest Human Herpes Virus-5 [33, 35]. Also, to curtail this deadly virus ravaging the globe, measures have been put in place to reduce the rate of transmission via social distancing, regular hand washing as well as the use of personal protective equipment like hand gloves and nose mask. However, repositioning old drugs whose safety profile, pharmacokinetics, side effects, drug interactions, and optimal dosage level are well known is an efficient tool in drug discovery [15, 20] especially with this fast-spreading pandemic.

Among the candidate drugs already considered for repositioning/repurposing against SARS-CoV-2 are chloroquine, azithromycin, remdesivir, lopinavir, favipiravir, ritonavir, ivermectin, and ruxolitinib. A considerable amount of literature has been published on the effect of chloroquine on SARS-CoV-2 [16]; these studies provide evidence for its effectiveness against SARS-CoV-2 virus replication. Clinical trials involving the use of azithromycin has also been reported [20]. In the same vein, remdesivir, favipiravir, and ivermectin, previously shown to possess broad-spectrum antiviral activity inhibit the SARS-CoV-2 virus in vitro [8, 59]. Ruxolitinib, lopinavir, and ritonavir (clinicaltrials.gov/ct2/show/NCT04334044) have been undergoing trials in the management of the SARS-CoV-2 virus [41].

Nevertheless, as the world is witnessing the second wave of the pandemic despite the available vaccines, the struggle of total apprehension of this critical situation of the world remains a major concern of drug design experts and researchers. The use of a mechanistic approach via Computer-Aided Drug Design (CADD) remains an indispensable in-silico method employed in every stage of the modern drug discovery process. It is used in the design of small-molecule ligands, identification & optimization of lead, and sorting-out of suitable drug candidates toward the development of new drug/vaccine [56]. However, various researchers have utilized this technique as a reliable mechanistic approach for exploring the inhibitory potential of a ligand against a target receptor during ligand-receptor interaction as seen in [1, 18, 32, 34, 36, 43–45, 53]. However, the “Molecular Docking Method” is a CADD approach that helps to understand potential drug-receptor

interactions in the active site of the target receptor. It shows how a potential drug candidate (ligand) obstructs the activities of the target receptor through the binding site responsible for biological and catalytic activities. Therefore, the present study is aimed at investigating the inhibitory potential of some selected antibiotics against the novel SARS-CoV-2 main protease (M^{pro}) via target-based drug discovery approach (virtual screening), drug-likeness analysis, oral-bioavailability studies, ADMET profiling, and bioactivity studies.

Materials and methods

Preparation of ligands

In this study, sixteen commercial antibiotics were used as ligands, while two clinically drugs (Remdesivir and Azithromycin) whose randomized clinical trials as probable inhibitors of SARS-CoV-2 main protease have been established were used as standards. The 3D structures of the ligands and standards were obtained from the PubChem database (<https://pubchem.ncbi.nlm.nih.gov>). The conformational search was performed using Spartan 14 Conformer Distribution with Molecular Mechanics/MMFF, and the most stable conformers were chosen and optimized. Optimization was carried out on Spartan 14' software using density functional theory (DFT) method with the B3LYP functional and the 6-31 + G (d) as the basis set.

Preparation of target receptor

SARS-CoV-2 M^{pro} (PDB ID: 6LU7) was used as the target receptor in this study. The crystal structure was retrieved from the protein data bank (RCSB) (<http://www.rcsb.org/pdb>). SARS-CoV-2(M^{pro}) [37] is an important protease that mediates replication and transcription of the virus in the host. It plays an indispensable regulatory function in SARS-CoV-2 infection, and progression [60], and has been widely reported as an important target enzyme in the development of anti-SARS-CoV-2 therapeutic agents as seen in [1, 12, 18, 32], therefore, it is an important and reliable enzyme and the main target of potential inhibitors. The co-crystallized (N3) molecules were removed to avoid any unwanted molecular interactions with the target receptor during virtual screening exercise using Biovia Discovery Studio [4]. The quality of the SARS-CoV-2 M^{pro} structure was validated using the Ramachandran plot (Fig. 1). The grid box (binding pocket) of the native ligand inhibitor used with the target receptor was employed as a basis to define the binding pocket for the X, Y, and Z coordinate as -26.284 , 12.603 and 58.96 respectively and

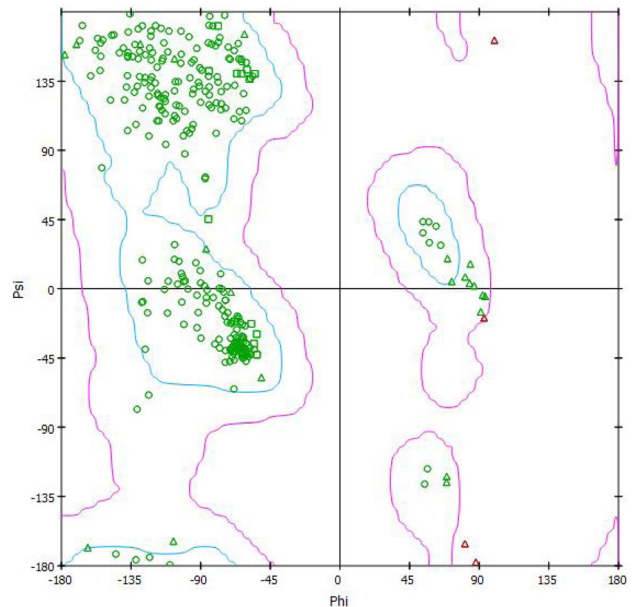


Fig. 1 The Ramachandran plot of SARS-CoV-2 M^{pro} (6LU7). Glycine = triangles, Squares = proline, All other residues = circles

the whole protease (target receptor) was enclosed in the grid.

Determination of (6LU7) M^{pro} active sites

Computed Atlas for Surface Topography of Proteins (CASTp) (<http://sts.bioe.uic.edu/castp/index.html?2011>) [55] and Biovia Discovery Studio (2019) were used to determine binding pocket, amino acids and all ligands interactions in the active site of SARS-CoV-2 M^{pro} . The result obtained was validated using experimental results reported for SARS-CoV-2 M^{pro} in complex with N3 native ligand [39].

Molecular docking simulation

Docking simulations of the optimized most stable conformers (ligands and standards) against the target receptor (SARS-CoV-2 M^{pro}) were done using Autodock (MGL tool- 1.5.6) and AutodockVina [58]. The inhibiting abilities of the ligands and standards against the target receptor using their respective binding affinities (kcal/mol) were assessed using Eq. 1, while other molecular interactions that occurred during the simulation were viewed using Biovia-2019 Discovery Studio [4].

$$K_i = 10^{(B.E./1.366)} \quad (1)$$

K_i is the inhibition constant in μM and B.E. is the binding energy in kcal/mol.

Assessment of pharmacokinetic properties

ADMET SAR2 [14] was used to predict the absorption, distribution, and metabolism and toxicity properties of the selected compounds. SwissADME webserver was used to investigate the oral bioavailability properties of the compounds while important features related to drug-likeness of the selected compounds were evaluated using Molinspiration online tool (<http://molinspiration.com/>).

Results and discussion

SARS-CoV-2 main protease (Mpro) structure and active gauge analysis

The structure of SARS-CoV-2 main protease (PDB ID: 6LU7) is shown in Table 1. 6LU7 is a 306 amino acid protease complexed with a native inhibitor N3 (N3-(N-[(5-Methylisoxazol-3-Yl) Carbonyl] Alanyl-L-Valyl-N¹~-(1r, 2z)-4-(Benzyloxy)-4-Oxo-1-[(3r)-2-Oxopyrrolidin-3-Yl] Methyl} But-2-Enyl)-L-Leucinamide). Its X-ray structure contains 23% α -helix, 31% β -sheets, 45% Coil and 28% Turns, with 2.16 Å resolution and crystal dimension of The study of its X-ray diffraction, a = 97.93 Å, b = 79.48 Å and c = 51.08 Å and angles α (900), β (114.550) and γ (900) respectively. 6LU7 has TASA (total accessible surface area) of 14,043(Å)² and

R-values (fee = 0.235, work = 0.202, and observed = 0.204).

The SARS-CoV-2 main protease has three domains with residues (8–110), (102–184) and (185–200) in domain 1, 2 and 3[39]. Its active site/binding region is located in the cleft between Domain 1 and 2. The gauge is characterized with Cys-His catalytic dyad [39] which is very essential to its catalytic and biological activities. This agrees with what has been reported earlier [18].

Molecular docking analysis

The Discovery and development of new therapeutic agents using the traditional method have been very challenging. It is very expensive, time-consuming, and with a low success rate, thus making the mechanistic approach i.e. the use of Computer-Aided Drug Design (CADD), an indispensable method. Recent developments in drug discovery/design have led to a renewed interest in this computational strategy (CADD), as it has been proved to easier, faster and cheaper with an outstanding success rate in the screening of molecules for biological and chemical interactions compared to the traditional methods [19]. It speeds up the process of designing small-molecule ligands, identification of lead and optimization and sorting out of drug candidates of best fit toward the development of novel therapeutic agents. Molecular docking is an important tool in computational drug discovery that provide predictive information

Table 1 The structure and active site of SARS-CoV-2 main protease (M^{pro}) in complex with N3 native ligand

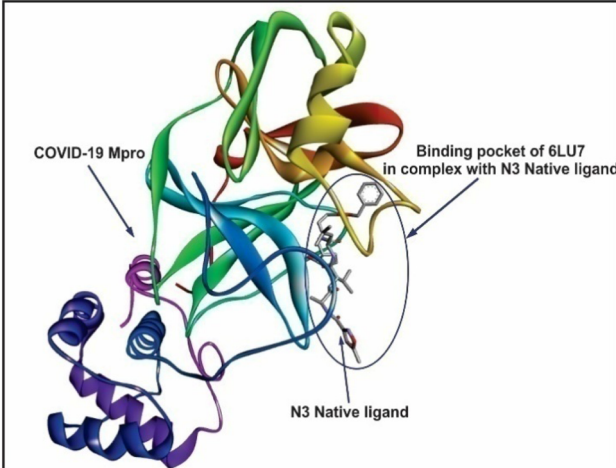
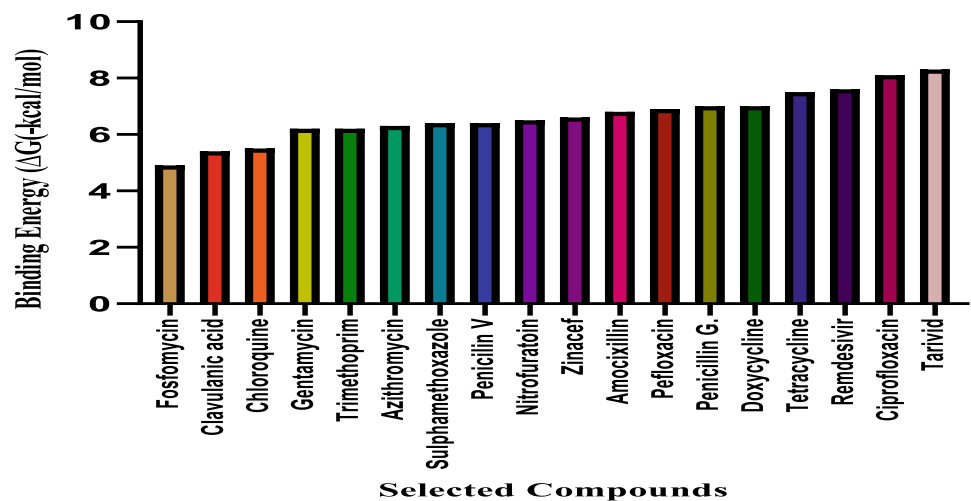
| PDB ID | Macromolecule and native ligand | Active site amino acids |
|--------|---|--|
| 6LU7 |  | Thr24, Thr25, Thr26, His41, Met49, Tyr54, Phe140, Leu141, Asn142, Gly143, Ser144, Cys145, His163, His164, Met165, Glu166, Leu176, Pro168, His172, Asp187, Arg188, Gln189, Thr190, Ala191, Gln192 |

Fig. 2 The bar chart showing the molecular docking scores between M^{Pro} (6LU7) and selected drug candidate compounds. (The value for binding energy (ΔG) is indicated in minus kcal/mol)



on the binding of small molecules to target receptor [40]. The molecular docking approach has found wide application because it offers predictions with a higher degree of accuracy of binding affinities, intermolecular interaction, and conformations of ligand's molecule at receptor's binding sites [19, 26, 40]. The docking scores of the ligands and standards against SARS-CoV-2 M^{Pro} (PDB ID: 6LU7) were as presented in Table 2. From the results, a good number of ligands displayed activity comparable to those of standards. Binding affinities for the standards range between -7.6 kcal/mol (Remdesivir) and -6.3 kcal/mol (Azithromycin) while those of the ligands were between -8.3 kcal/mol and -4.9 kcal/mol. Overall, tarivid with binding affinity -8.3 kcal/mol had the most outstanding inhibitory activity, amino acids involved in its hydrogen bond interaction with receptor molecules are Glu166, Tyr54, Asp187, and Met49, while electrostatic/hydrophobic interactions include Phe140, Asn142, His41, Met165, Arg188. It is interesting to note that tarivid (ofloxacin) and ciprofloxacin displayed better inhibitory activity against SARS-CoV-2 virus M^{Pro} (as shown by the binding affinity and inhibition constant) than remdesivir even though more recovery rate had recently been recorded in the use of the latter but not without some fatality and side effects (<https://www.nature.com/articles/d41586-020-01295-8>). The high binding affinity recorded, could be attributed to the multiple hydrogens, electrostatic and hydrophobic bonds involved in binding to amino acids at the active site of SARS-CoV-2 M^{Pro}. Tetracycline also demonstrated inhibitory activity almost equal in strength to remdesivir against SARS-CoV-2 while doxycycline and Penicillin G inhibited the virus much better than Azithromycin. To validate the significance of using in-silico approach to elucidate the binding affinity and interactions of ligands to the receptor as reported above, it worthy of mentioning that this method has been widely used in

notable research in the studies and design of therapeutic agents for viral diseases as observed in [1, 31, 50].

More recently, literature has emerged on the potential of tetracycline in the treatment of COVID-19 and this has further supported findings from this study [51]. Other ligands used in this study displayed notable inhibition better than azithromycin. The inhibition potential of the drugs as ranked by the binding affinity (Fig. 2) and inhibition constant are as shown below.

Tarivid > Ciprofloxacin > Remdesivir > Tetracycline > Doxycycline = Penicillin G > Pefloxacin > Amoxicillin > Zinacef > Nitrofurantoin > Sulphamethoxazole > Penicillin V > Azithromycin > Trimethoprim = Gentamycin > Chloroquine > Clavulanic Acid > Fosfomycin.

This study furnishes tarivid, ciprofloxacin, tetracycline, and doxycycline (Figs. 3 and 4) as significant potential inhibitors of SARS-CoV-2 as compared to remdesivir and zithromycin. Tarivid (ofloxacin) and ciprofloxacin are fluoroquinolones, with good oral and pharmacokinetic properties, they demonstrated broad-spectrum activity against bacterial infections including lower and upper respiratory tract infections (RTI) [24], the efficacy of cef-tazidime and ciprofloxacin in clinical trials involving RTI patients has been reported in the literature, although, cef-tazidime was not as effective as ciprofloxacin [30].

Drug-likeness and oral bioavailability analysis of the selected compounds and standards

Analysis of the pharmacokinetic properties of potential drug candidates is very essential in the early stage of drug discovery. According to Lipinski and his team, drug-like compounds must obey the rule of five (RO5) i.e. molecular weight (MW) ≤ 500 Da, number of hydrogen bond donor (HBD's) ≤ 5 , number of hydrogen bond acceptor

Table 2 Docking scoring, binding sites, hydrogen bond distances and the inhibition constants of the interaction of selected antibiotics and standard drugs with SARS-CoV-2(M^{pro}) (PDB ID: 6LU7), a prominent target receptor of inhibitors of the Severe Acute Respiratory Syndrome Coronavirus (SARS-CoV-2)

| Ligands | Binding Affinity (ΔG), kcal/mol | 6LU7 Receptor amino acids forming H-bond with ligands (H-bond Distance, Å) | Electrostatic/ Hydrophobic Interactions involved | Inhibition Constant (K_i), μM |
|------------------|---|--|--|--|
| Tarivid | - 8.3 | Glu166 (2.0 Å), Tyr54 (2.8 Å) Asp187 (3.0 Å), Met49 (3.3 Å) Glu166 (3.6 Å) | Phe140, Asn142, His41, Met165, Arg188 | 0.83 |
| Ciprofloxacin | - 8.1 | Phe140 (2.5 Å), Tyr54 (2.8 Å) Asp187 (3.1 Å), Gln189 (3.1 Å) | Met49, Met165, His41, Cys145, Asn142, Leu141 | 1.16 |
| Remdesivir | - 7.6 | Lys137 (2.3 Å), Thr199 (2.4 Å), Arg131 (2.5 Å), Asn238 (2.6 Å), Thr199 (3.2 Å), Glu290 (3.3 Å), Thr198 (3.4) | Leu286, Asp289, Asp197 | 2.70 |
| Tetracycline | - 7.5 | Cys145 (2.1 Å), Thr26 (2.4 Å), Thr26 (2.6 Å), Ser144 (2.8 Å), Thr26 (2.9 Å), Thr26 (3.1 Å), Leu141 (3.1 Å), Thr24 (3.1 Å), Thr24 (3.1 Å) | Gly143 | 3.2 |
| Doxycycline | - 7.0 | Thr190 (2.2 Å), Glu166 (3.0 Å), Gln189 (3.0 Å), His164 (3.0 Å) | Leu167, Pro168, Cys145 | 7.43 |
| Penicillin G | - 7.0 | Gln110 (2.1 Å), Arg105 (3.0 Å), Thr111 (3.3 Å) | Val104, Phe294 | 7.43 |
| Pefloxacin | - 6.9 | Gly143 (2.2 Å), Ser144 (2.4 Å), Cys145 (2.5 Å), His163 (2.8 Å), Leu141 (2.9 Å), Asn142 (3.5 Å) | Glu166, Thr190 | 8.80 |
| Amoxicillin | - 6.8 | Leu272 (3.0 Å), Leu271 (3.0 Å), Asp289 (3.0 Å), Thr199 (3.3 Å), Arg131 (2.6 Å) | Leu286, Tyr237 | 10.41 |
| Zinacef | - 6.6 | Gly143 (2.3 Å), Thr26 (2.3 Å), Glu166 (2.5 Å), Asn142 (3.0 Å), Leu141 (2.9 Å), Leu141 (3.1 Å), Thr26 (3.2 Å), Thr24 (3.3 Å), Thr26 (3.5 Å) | His41 | 14.59 |
| Nitrofurantoin | - 6.5 | Ser144 (1.8 Å), Cys145 (2.3 Å) Ser144 (2.3 Å), Gly143 (2.5 Å), Phe140 (3.3 Å) | His41 | 17.27 |
| Sulfamethoxazole | - 6.4 | Gln110 (2.0 Å), Thr111 (2.1 Å), Asp153 (2.5 Å), Asn151 (3.1 Å), Thr111 (3.4 Å) | Val104, Phe294 | 20.45 |
| Penicillin V | - 6.4 | Gly143 (2.2 Å), Thr26 (2.8 Å), Gln189 (3.3 Å) | Met165, His164, His41, Met49 | 20.45 |
| Azithromycin | - 6.3 | Asp197 (3.0 Å), Tyr237 (3.0 Å), Asp289 (3.5 Å) | Met276, Leu286, Leu287, Tyr239 | 24.20 |
| Gentamycin | - 6.2 | Thr337 (2.1 Å), Leu287 (2.2 Å), Asn238 (2.2 Å), Asn238 (2.6 Å), Asp197 (2.8 Å), Asp197 (3.2) | Nil | 28.65 |
| Trimethoprim | - 6.2 | His163 (2.1 Å), Asn142 (2.2 Å), Glu166 (2.4 Å), Phe140 (2.5) | Leu141, Met165, Cys145, His41 | 28.65 |
| Chloroquine | - 5.5 | His164 | Asn142, His41, Met165 | 93.34 |
| Clavulanic Acid | - 5.4 | His163 (2.0 Å), Ser144 (2.2 Å), Cys145 (2.4 Å), Leu141 (2.9 Å), Phe140 (3.0 Å), Glu166 (3.2 Å), Leu141 (3.3 Å), Asn142 (3.3 Å) | Met165 | 110.50 |
| Fosfomycin | - 4.9 | Thr111 (1.9 Å), Gln110 (2.1 Å), Gln110 (2.4 Å), Thr111 (2.8 Å), Asn151 (2.9 Å), Thr111 (3.1 Å) | Phe294, Asp295 | 256.86 |

Table 3 Drug-likeness evaluation of the significant antibiotics and standards using Molinspiration online tool

| Compounds | Heavy atoms (HA) | Molecular weight (MW) | RO5 Violations | Hydrogen bond donor (HBD) | Hydrogen bond acceptor (HBA) | miLog P |
|-----------|------------------|-----------------------|----------------|---------------------------|------------------------------|---------|
| C-1 | 26 | 361.37 | 0 | 1 | 7 | - 0.26 |
| C-2 | 24 | 331.35 | 0 | 2 | 6 | - 0.70 |
| C-3 | 32 | 444.44 | 1 | 7 | 10 | - 0.24 |
| C-4 | 32 | 444.44 | 1 | 7 | 10 | - 0.43 |
| S-1 | 42 | 602.59 | 2 | 5 | 14 | 2.82 |
| S-2 | 52 | 749.00 | 2 | 5 | 14 | 2.73 |

Table 4 Oral bioavailability analysis of the selected compounds and standards using SwissADME

| Ligand | C-1 | C-2 | C-3 | C-4 | S-1 | S-2 |
|-------------------------|--|--|---|---|---|--|
| Formula | C ₁₈ H ₂₀ FN ₃ O ₄ | C ₁₇ H ₁₈ FN ₃ O ₃ | C ₂₂ H ₂₄ N ₂ O ₈ | C ₂₂ H ₂₄ N ₂ O ₈ | C ₂₇ H ₃₅ N ₆ O ₈ P | C ₃₈ H ₇₂ N ₂ O ₁₂ |
| VINA Score | - 8.3 | - 8.1 | - 7.5 | - 7.0 | - 7.6 | - 6.3 |
| Mass | 361.37 | 331.34 | 444.43 | 444.43 | 602.58 | 748.98 |
| TPSA | 75.01 | 74.57 | 181.62 | 181.62 | 213.36 | 180.08 |
| #Rotatable bonds | 2 | 3 | 2 | 2 | 14 | 7 |
| XLOGP3 | - 0.39 | - 1.08 | - 1.30 | 0.54 | 1.91 | 4.02 |
| WLOGP | 1.2 | 1.18 | - 0.32 | - 0.5 | 2.21 | 1.52 |
| ESOL Log S | - 1.99 | - 1.32 | - 1.78 | - 2.94 | - 4.12 | - 6.55 |
| ESOL class | Very soluble | Very soluble | Very soluble | Soluble | Moderately soluble | Poorly soluble |
| Lipinski #violations | 0 | 0 | 1 | 1 | 2 | 2 |
| Bioavailability Score | 0.55 | 0.55 | 0.11 | 0.11 | 0.17 | 0.17 |
| PAINS #alerts | 0 | 0 | 0 | 0 | 0 | 0 |
| Brenk #alerts | 0 | 0 | 1 | 1 | 1 | 0 |
| Fraction Csp3 | 0.44 | 0.41 | 0.41 | 0.41 | 0.48 | 0.97 |
| Synthetic accessibility | 3.63 | 2.51 | 5.04 | 5.25 | 6.33 | 8.91 |

Table 5 Bioactivity analysis of the selected compounds and standards

| Bioactivity | C-1 | C-2 | C-3 | C-4 | S-1 | S-2 |
|--|---------|---------|---------|---------|--------|--------|
| AutoDockVina docking score (kcal/mol) | - 8.3 | - 8.1 | - 7.5 | - 7.0 | - 7.6 | - 6.3 |
| Ki (μM) | 0.83 | 1.16 | 3.2 | 7.3 | 2.70 | 24.20 |
| miLog P | - 0.26 | - 0.70 | - 0.24 | - 0.43 | 2.82 | 2.73 |
| Ligand efficiency (LE) /kcal/mol/heavy atom) | 0.319 | 0.338 | 0.234 | 0.219 | 0.180 | 0.121 |
| LE-scale | 0.380 | 0.404 | 0.316 | 0.316 | 0.229 | 0.161 |
| Fit quality (FQ) | 0.80 | 0.80 | 0.74 | 0.692 | 0.787 | 0.752 |
| Ligand-efficiency-dependent lipophilicity (LELP) | - 0.815 | - 2.071 | - 1.025 | - 1.963 | 15.667 | 22.561 |

C-1 = Tarivid, C-2 = Ciprofloxacin, C 3 = Tetracycline, C-4 = Doxycycline, S-1 = Standard 1 (Remdesivir), S-2 = Standard 2 (Azithromycin)

Table 6 ADMET prediction of selected compounds

| Parameters | C-1 | C-2 | C-3 | C-4 | S-1 | S-2 |
|--------------------------------|-----------------------------|-----------------------------|-----------------------------|----------------------------|----------------------------|----------------------------|
| <i>Absorption/distribution</i> | | | | | | |
| BBB (±) | 0.9680 (BBB +) | 0.3324 (BBB-) | 0.9939 (BBB-) | 0.9930 (BBB-) | 0.9625 (BBB +) | 0.9930 (BBB-) |
| HIA(±) | 0.9903 HIA + (99.03%) | 0.9807 HIA + (98.07%) | 0.9864 HIA + (98.64%) | 0.9885 HIA + (98.9%) | 0.9135 HIA + (91.4%) | 0.6142 IA- (61.42%) |
| Aqueous Solubility(LogS) | - 3.511 | - 3.464 | - 3.071 | - 3.057 | - 3.474 | - 2.06 |
| <i>Metabolism</i> | | | | | | |
| CYP450 2C19 Inhibitor | 0.9026 Non-Inhibitor | 0.9025 Non-Inhibitor | 0.9099 Non-Inhibitor | 0.9089 Non-Inhibitor | 0.7362 Non-Inhibitor | 0.9023 Non-Inhibitor |
| CYP450 1A2 Inhibitor | 0.9045 Non-Inhibitor | 0.7735 Non-Inhibitor | 0.9045 Non-Inhibitor | 0.9046 Non-Inhibitor | 0.7447 Non-Inhibitor | 0.9295 Non-Inhibitor |
| CYP450 3A4 Inhibitor | 0.8309 Non-Inhibitor | 0.8309 Non-Inhibitor | 0.8567 Non-Inhibitor | 0.8686 Non-Inhibitor | 0.7224 Non-Inhibitor | 0.9533 Non-Inhibitor |
| CYP450 2C9 Inhibitor | 0.9070 Non-Inhibitor | 0.9070 Non-Inhibitor | 0.9144 Non-Inhibitor | 0.9071 Non-Inhibitor | 0.7246 Non-Inhibitor | 0.9021 Non-Inhibitor |
| CYP450 2D6 Inhibitor | 0.9268 Non-Inhibitor | 0.9231 Non-Inhibitor | 0.9293 Non-Inhibitor | 0.9231 Non-Inhibitor | 0.8503 Non-Inhibitor | 0.8904 Non-Inhibitor |
| <i>Excretion</i> | | | | | | |
| Biodegradation* | 0.9500 NB | 0.8500 NB | 0.9750 NB | 0.9750 NB | 0.7750 NB | 0.8250 NB |
| <i>Toxicity</i> | | | | | | |
| AMES toxicity | 0.7300 Non-Ames Toxic | 0.8900 Ames Toxic | 0.6300 Non-Ames Toxic | 0.7200 Non-Ames Toxic | 0.7400 Non-Ames Toxic | 0.8300 Non-Ames Toxic |
| Acute oral toxicity | 0.7916 III | 0.7731 III | 0.7981 III | 0.7834 III | 0.5357 III | 0.7761 III |
| Eye irritation (YES/NO) | NO | NO | NO | NO | NO | NO |
| Eye corrosion (YES/NO) | NO | NO | NO | NO | NO | NO |
| hERG Inhibition | 0.8179 NO | 0.8225 NO | 0.3636 NO | 0.3965 NO | 0.5000 NO | 0.6048 NO |
| carcinogenicity | 0.7286 Non-Carcinogenic | 0.8043 Non-Carcinogenic | 0.8539 Non-Carcinogenic | 0.9429 Non-Carcinogenic | 0.9714 Non-Carcinogenic | 0.9857 Non-Carcinogenic |

*NB: Not biodegradable

C-1 = Tarivid, C-2 = Ciprofloxacin, C-3 = Tetracycline, C-4 = Doxycycline, S-1 = Standard 1 (Remdesivir), S-2 = Standard 2 (Azithromycin)

(HBAs) ≤ 10 and octanol–water partition coefficient (Log P) ≤ 5 and no more than one violation is allowed [38]. As shown in Table 3, the HA, MW, HBD, HBA, and Log P values of all the selected compounds are within the acceptable range as stated in the RO5 and no compound violate more than one rule, whereas, the two standard drugs used (Remdesivir, S-1, and Azithromycin, S-2) have two violations respectively.

The oral bioavailability and other physicochemical properties of the selected compounds and standards

obtained using the SwissADME web tool are shown in Table 4. The bioavailability radar (Fig. 5) gives a swift catch sight of the important physicochemical properties and drug-likeness of the selected compounds and standards [17]. As shown in (Fig. 5), the coloured portion (Pink) shows the most desirable area for each of the bioavailability properties (LIPO, SIZE, INSOLU, POLAR, INSATU, and FLEX). The octanol–water partition coefficient (XLOGP3) (Table 4) was used to determine the LIPO (Lipophilicity) of the selected compounds and standards.

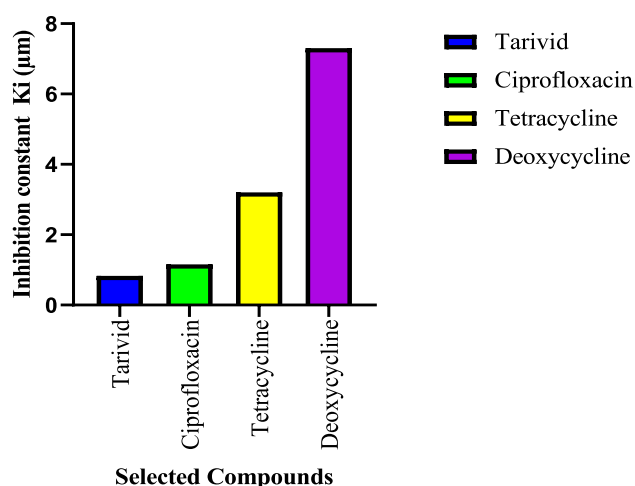
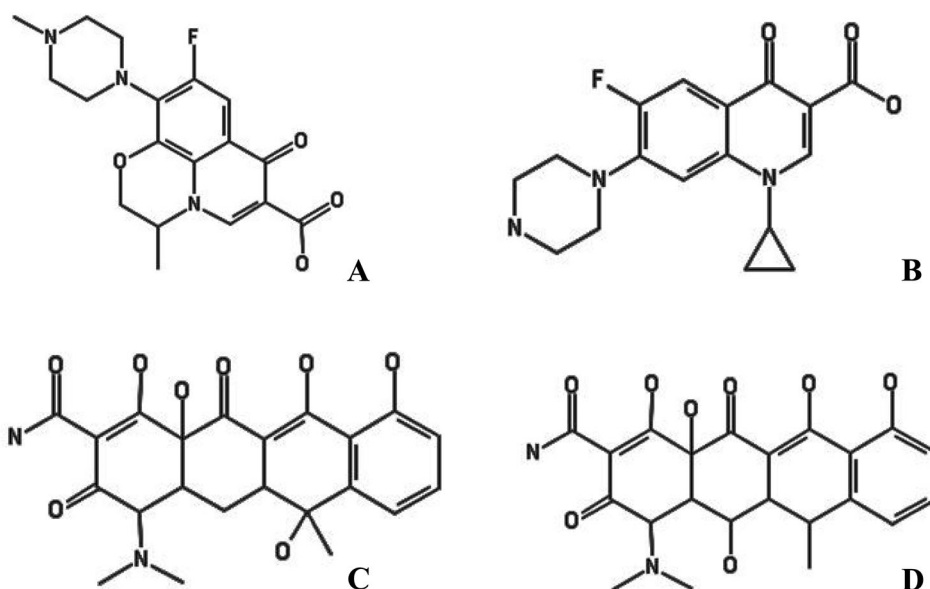


Fig. 3 The bar chart showing the selected Antibiotics as a significant potential inhibitor of SARS-CoV-2M^{Pro}

Surprisingly, all the selected compounds and standards were in the coloured region and fall within the LIPO recommended range of -0.7 to $+5.0$. According to Lipinski rule of five (RO5), the SIZE (Molecular Weight) of a good drug candidate is expected not to be more than 500gmol^{-1} , of which of all selected compounds (C-1 to C-4) obey except the two standards ($S-1 = 602.58$, $S-2 = 748.98$). The INSOLU (insolubility) requirement of the selected compounds and standards as depicted in their ESOL (Log S) and ESOL Class revealed that C-1, C-2, and C-3 are very soluble, while C-4 is soluble and S-1 and S-2 are moderately soluble and insoluble respectively. The Total Polarity Surface Area (TPSA) whose recommended value is between the range of 20 and 130 \AA^2 was used to examine the POLAR (polarity) of the selected compounds

Fig. 4 The Structures of Selected Compounds **a** Tarivid, **b** Ciprofloxacin, **c** Tetracycline, **d** Doxycycline



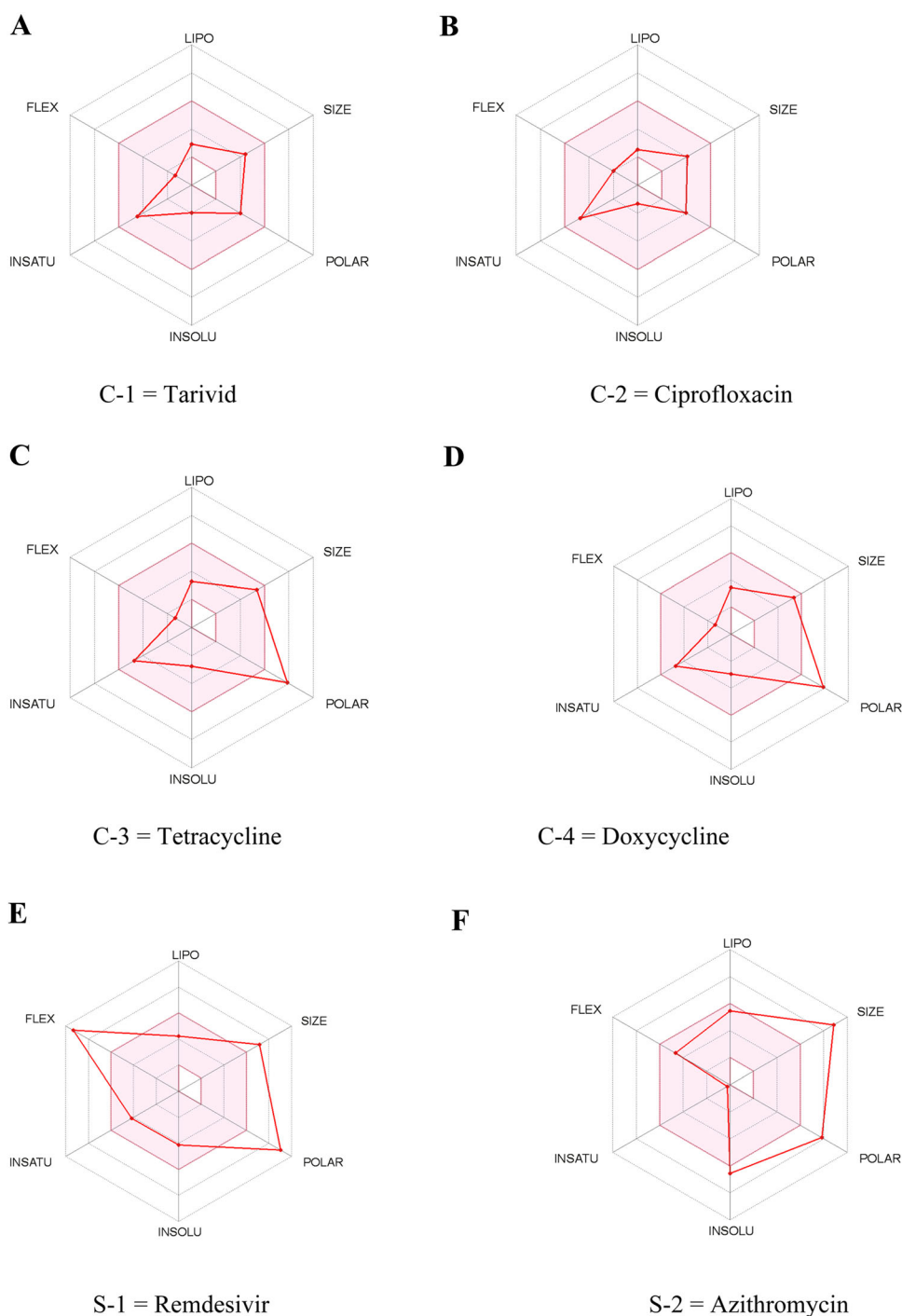
and standards. As shown in Table 4 and Fig. 5, only C-1 and C-2 fall within the optimal range while others fell apart. The fraction of carbon Sp³ (CSP³) which is expected to be the range of 0.25 and 1 and the number of the rotatable bond which should not exceed nine are used to determine the INSATU (unsaturation) and FLEX (flexibility) of the selected compounds are standards. Interestingly, all the selected compounds fall within the INSATU recommended range of values while only Remdesivir (S-1) disobey the FLEX requirement. Put together, Tarivid (C-1) and Ciprofloxacin (C-2) have the best oral bioavailability since all their physicochemical properties fall within the optimal coloured (pink) region.

Bioactivity of the selected compounds and standards

The bioactivity properties of the selected Antibiotics are summarized in Table 5. The relationship between the docking score and binding affinity confirmed its usage in calculating the inhibition constant (K_i) using (Eq. 1). For a compound to be a Hit, its K_i value should be a micro-molar range of 0.1 – $1.0 \mu\text{M}$ and not more than 10 nM for a drug [5, 27, 49, 52]. Also, the lower values of K_i indicate better inhibitory activity [6]. The inhibition constant values of the significantly selected antibiotics range from (0.83 – $7.43 \mu\text{M}$).

From Table 5, both C-1 ($0.83 \mu\text{M}$) and C-2 (1.16) are qualified as Hit while C-1 is the most potent of all the selected compounds. For other bioactivity parameters like Ligand Efficiency (LE), Fit Quality (FQ), and Ligand-efficiency-dependent lipophilicity (LELP) (Eq. 2–5), their recommended values for a hit are ≥ 0.3 , ≥ 0.8 and -10 to 10 respectively [25, 48]. Similarly, the (LE), (FQ) and

Fig. 5 The bioavailability radar for the selected compound. Pink area = Most desirable area for each of the bioavailability properties, LIPO = Lipophilicity, POLAR = Polarity, INSOLU = Insolubility, FLEX = Flexibility, SIZE = Molecular weight, INSATU = Unsaturation



(LELP) values observed for C-1 and C-2 are within the recommended range, although all the selected compounds obey (LELP) recommended value except S-1 and S-2 with LELP values of 15.667, and 22.5619 respectively (see Table 5).

$$K_i = e^{\left[\frac{-\Delta G}{RT}\right]} \quad (2)$$

where R = Gas constant (1.987×10^{-3} kcal/K-mol);

T = 298.15 (Absolute Temperature); k_i = Inhibition constant

$$\text{Ligand Efficiency (LE)} = -B.E \div \text{Heavyatoms (H.A)} \quad (3)$$

$$LE_{scale} = 0.873e^{-0.026 \times H.A} - 0.064 \quad (4)$$

$$FQ = LE \div LE_{scale} \quad (5)$$

$$LELP = \text{LogP} \div LE \quad (6)$$

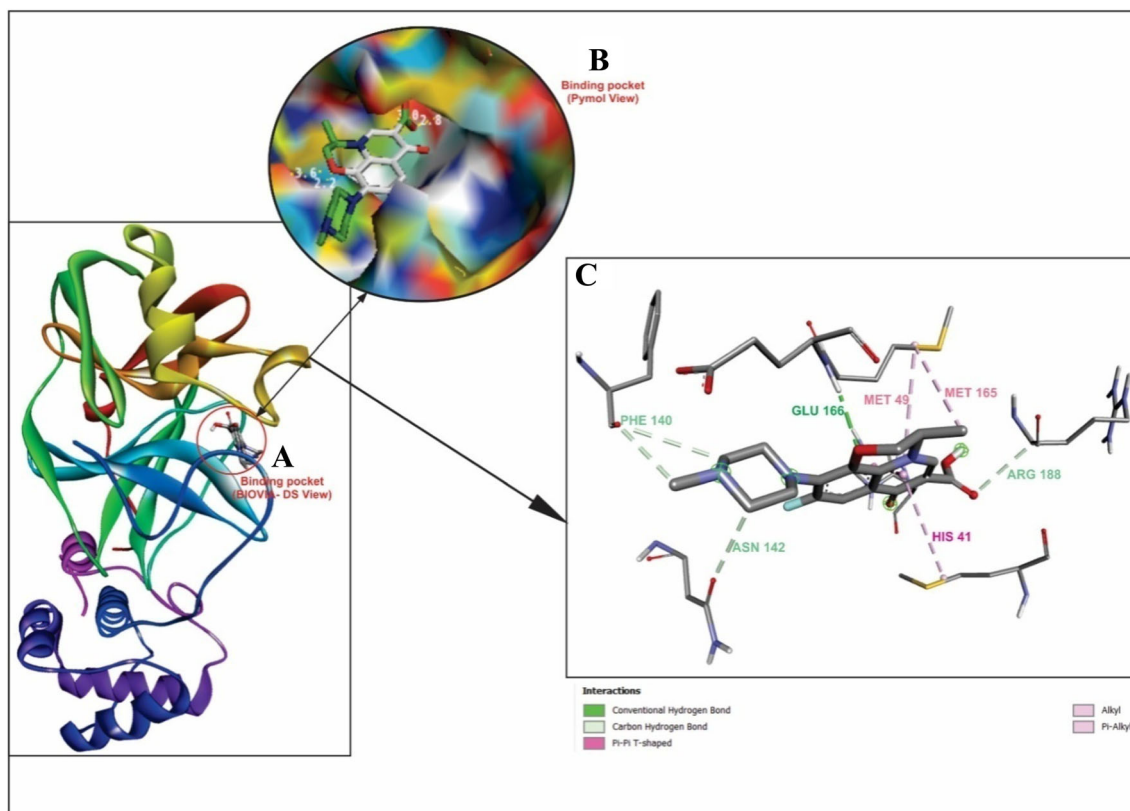


Fig. 6 The binding pockets (a, b) and binding mode (c) of C-1 (Tarivid) with amino acids in SARS-CoV-2M^{PRO} (6LU7)

ADMET properties of the selected compounds and standards

The results of ADMET (absorption, distribution, metabolism, excretion, and Toxicity) shown in Table 6 are computed using the ADMETSAR2 web server [14]. ADMET properties play significant roles in the early stage of drug discovery and development since high-quality drug candidates are to possess both sufficient efficacies against the therapeutic target as well as appropriate ADMET properties at a therapeutic dose [23]. Interestingly, all the selected Antibiotics and standards have an excellent probability of being absorbed in the human intestine with HIA + values of 99.03%, 98.07%, 98.64%, 98.9% and 91.4% for C-1, C-2, C-3, C-4, and S-1 respectively, except S-2 with HIA- (61.42%). Also, C-1 and S-1 have an excellent probability of crossing the blood–brain barrier (BBB + 96.8% and 96.3% respectively), an important pharmacokinetic property in drug discovery. Other selected drug candidates and standard show negative BBB potential; although this may not be a threat since our focus in this study is not directed towards finding potential drug candidates that target receptors in the brain, like antipsychotics, antiepileptic, and antidepressant drugs do. Furthermore, a drug molecule is

expected to be in an aqueous solubility range of -1 to -5 [3] and the Log S values of all the selected Antibiotics and standards fall within the range, indicating that the selected Antibiotics have good absorption and distribution potential.

Furthermore, microsomal enzymes (Cytochrome P450 inhibitors) were used to predict the metabolic activities of the selected drug candidates. All the selected drugs and standards are non-inhibitors of all the cytochrome P450 which enhances their metabolism as potential therapeutic drugs. Although all the selected Antibiotics and standards are predicted to be non-biodegradable nevertheless, they are non-carcinogenic. Considering the AMES toxicity of the selected Antibiotics and standards i.e. their mutagenic abilities, all except compound C-2 are non-AMES-toxic. Also, all the selected compounds and standards possess type III oral acute toxicity indicating that they are slightly toxic although they show no eye irritation and corrosion. However, type III toxicity can easily be upgraded to type IV and become (non-toxic) during the lead optimization stage of drug discovery [44]. The ability of a drug molecule to inhibit human ether a-go-go (hERG) is very dangerous, as it can lead to blockage of the potassium ion channel of the myocardium which disrupts the electrical activity of the heart and may result in untimely death [47]. Interestingly, all the selected Antibiotics and standards are non-inhibitor

of hERG with compound C-1 and C-2 having the better potential of being non-inhibitor of hERG. Summarily, all the selected compounds are safer and excellent drug candidates against the target receptor.

Binding modes and molecular interactions

The binding mode and molecular interactions give more information on the interacting mode of the selected Antibiotics with a bond to the main protease (M^{pro}). Since compound C-1 and C-2 give better inhibitory potential and promising physicochemical and bioactivity properties among the four selected compounds, only their binding mode and molecular interactions are discussed. As shown in Figs. 6 and 7, the binding modes of the two selected hit compounds (C-1 and C-2) and fully embedded in the binding pocket located at the cleft between domains I and II which is the active site of the target protease (M^{pro}) (see Table 1). The non-bonded molecular interactions of C-1 (Fig. 8) as seen in AutoDock Vina docking results include Conventional Hydrogen Bond with Glu166, Carbon-Hydrogen Bond with Phe140, Asn142 and Arg188, Pi-Pi T-Shaped with His41 and Alkyl and Pi-Alkyl interactions with Met49 and Met165. Similarly, C-2 (Fig. 7) form Conventional Hydrogen Bond with Gln189, Glu166 and

Phe140, Carbon-Hydrogen Bond with Leu141, and Asn142, Pi-Pi T-Shaped interaction with His41 and Alkyl and Pi-Alkyl interactions with Cys145, Met49 and Met145. However, the presence of His41, Met49, Phe140, Asn142, Met165, and Glu166 amino acid residues in both compounds (C-1 and C-2) established that the two compounds have a similar binding pocket and confirmed the similarity in their mode of interactions. Various interactions exhibit by other selected compounds (C-3 and C-4) are shown in (Fig. 8). Finally, a close examination of the amino acid residues obtained in the interactions of C-1, C-2, C-3 and C-4 (Fig. 8), and the amino acids in the active site (Table 2) affirmed that all the selected antibiotics share the same binding pocket with N3 native ligand, although C-1 (Tarivid) and C-2 (Ciprofloxacin) are more potent and interact better with target receptor (M^{pro}).

In conclusion, as the world enters the second wave of the global pandemic (COVID-19) with no officially approved drug to apprehend the disease, the need for improving on intensive research through screening of phytochemicals, laboratory synthesis of novel drug candidates and repurposing odd drugs among other means becomes a necessity. Computer-Aided Drug Design (CADD) is an indispensable tool to accelerate the discovery and development of a new therapeutic agent to cure this

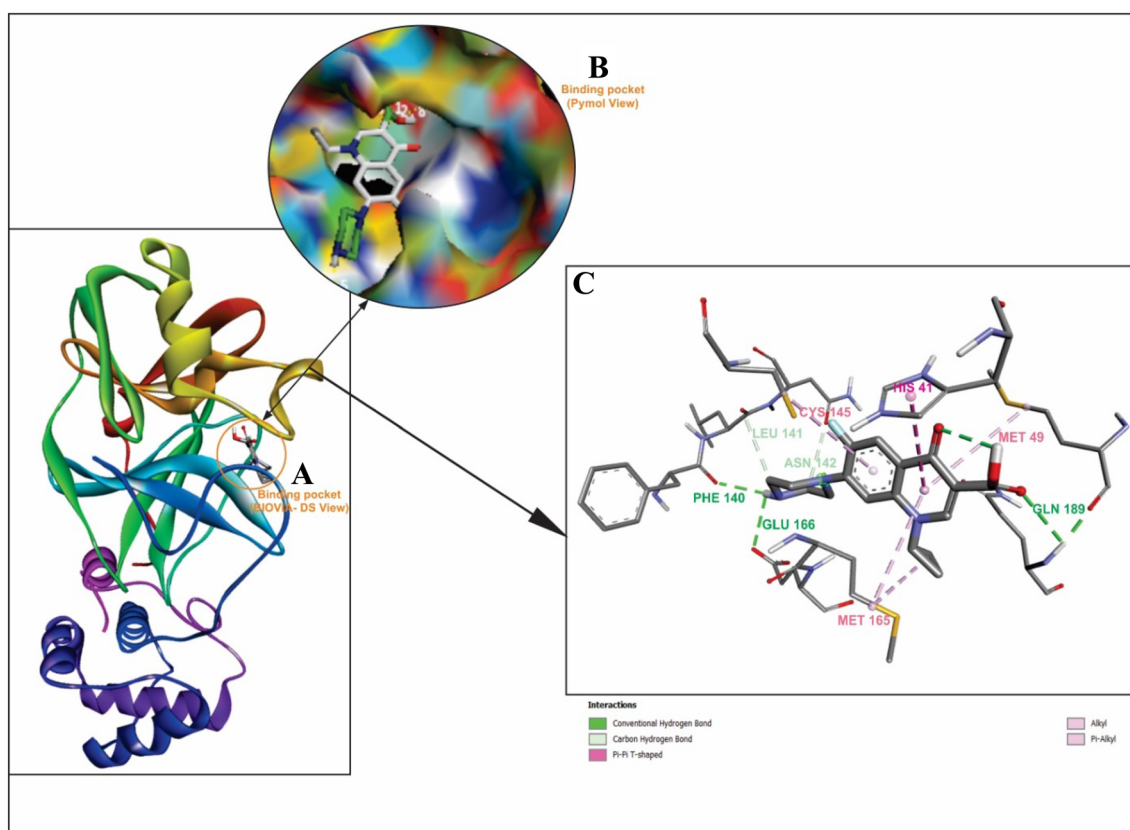


Fig. 7 The binding pockets (a, b) and binding mode (c) of C-2 (Ciprofloxacin) with amino acids in SARS-CoV-2 M^{pro} (6LU7)

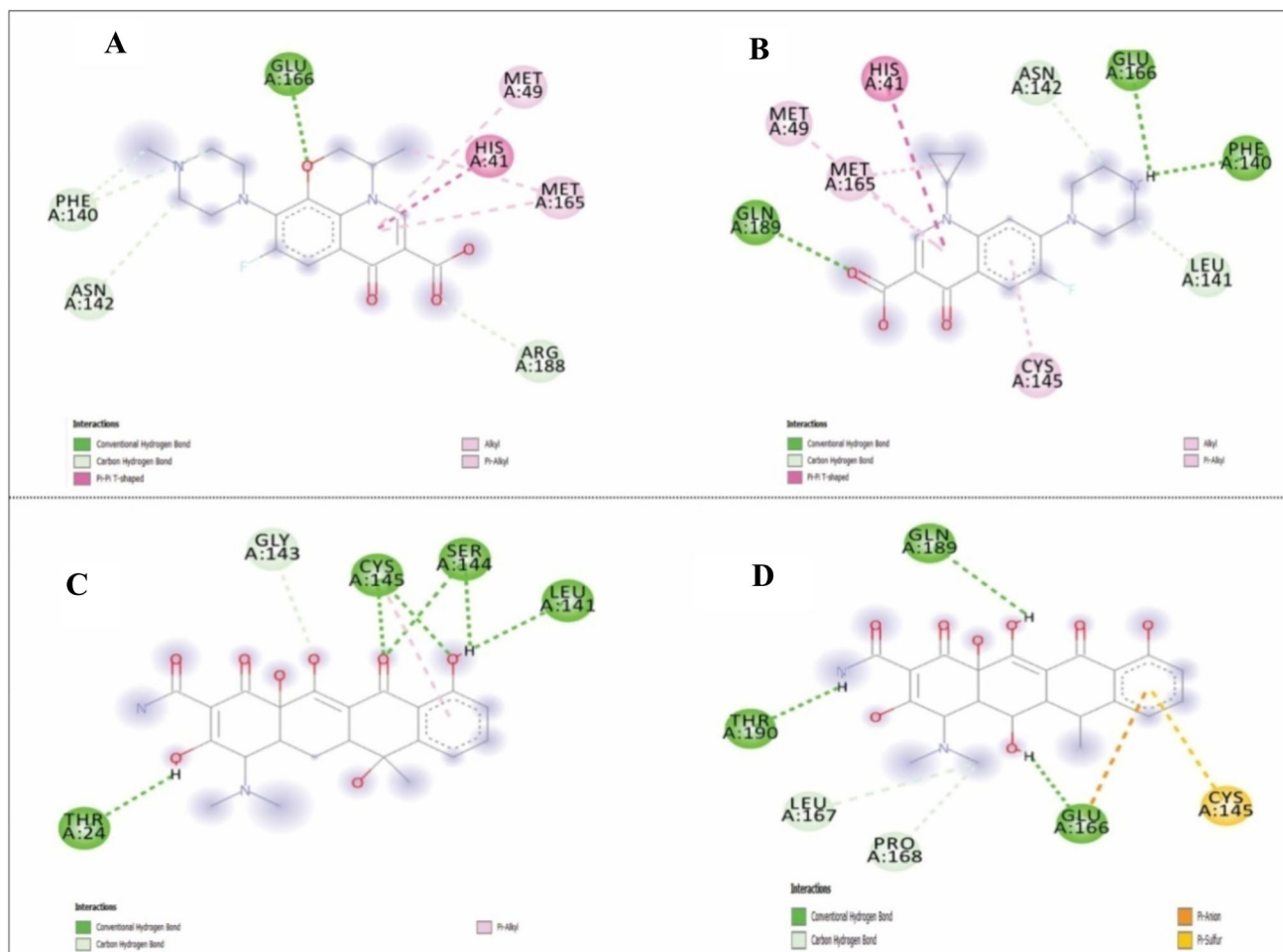


Fig. 8 The molecular interactions of C-1 (Tarivid), C-2 (Ciprofloxacin), C-3 (Tetracycline) and C-4 (Doxycycline) with amino acids in SARS-CoV-2M^{PRO} (6LU7)

lingering disease that has claimed lives in millions. It is a mechanistic tool widely used in all stages of the modern drug discovery process, for the design of small-molecule ligands, hit identification, lead optimization and selection of suitable drug candidate toward the development of a new therapeutic agent. The molecular Docking method, an indispensable CADD approach helps to study drug-receptor interactions in the active/binding site of the target receptor. It shows how the potential drug candidates (ligands) inhibit the replication and transcription of the target receptor in its active gauge where biological and catalytic activates takes place. Some drugs have been proved and approved to be effective for curing more than one disease. Therefore, the current research used CADD approach via molecular docking coupled with other relevant analyses to screen some commercial antibiotics against SARS-CoV-2 main protease (M^{PRO}) (6LU7). This study identified two antibiotics (Tarivid and Ciprofloxacin) as probable inhibitors of the target receptor responsible for replication and transcription of the virus. As reported by Burlingham and

Widlanski, 2003, compound with lower inhibition constant value has higher inhibitory efficiency, thus, the binding affinities(kcal/mol) and inhibition constant(μM) of both compounds (Tarivid, $- 8.3$ kcal/mol, 0.83 μM) and (Ciprofloxacin, $- 8.1$ kcal/mol, 1.16 μM) obtained from their interaction with the active site of the target receptor qualified them as hits. The two hit compounds interacted and shared the same pocket with the active site of the receptor located at the cleft between domains I and II. Both compounds obeyed the drug-likeness rule (RO5 rule of Lipinski) and show outstanding bioactivity and oral-bioavailability properties as compared to the two standards (Remdesivir and Azithromycin) whose randomized clinical trials have been completed [28]. Also, ADMET profiling of the two hits revealed their ability to be absorbed easily in the human intestine. Both are non-inhibitors of cytochrome P450, non-carcinogenic and non-hERG inhibitors, although, their potency, efficacy, pharmacokinetics and reduced toxicity can be improved during the Hit-Lead optimization stage of drug discovery, while molecular

dynamics and free energy calculation could be employed for further stability studies. The importance of in vivo and in vitro experiments to further establish the potency of the two hits compounds are fully acknowledged, but lack of financial aid limited our scope. We thereby recommend these two hit compounds for further experimental studies and clinical trials in the quest of finding a lasting solution to the ravaging pandemic (COVID-19).

Acknowledgements The authors wish to acknowledge members of the Computational and Biophysical Chemistry group in the Department of Pure and Applied Chemistry, Ladoko Akintola University of Technology, LAUTECH, Ogbomosho, Nigeria.

Funding No funding was received for conducting this study.

Declarations

Conflict of interest The authors have no conflicts of interest to declare that are relevant to the content of this article.

References

- Abdul-Hammed M, Adedotun IO, Olajide M, Irabor CO, Afolabi TI, Gbadebo IO, Rhyman L, Ramasami P. Virtual screening, ADMET profiling, PASS prediction, and bioactivity studies of potential inhibitory roles of alkaloids, phytosterols, and flavonoids against COVID-19 main protease (M^{pro}). *Natl Prod Res*. 2021. <https://doi.org/10.1080/14786419.2021.1935933>.
- Adedeji WA. The treasure called antibiotics. *Ann Ibadan Postgrad Med*. 2016;14:56–7.
- Bergenheim N. Preclinical candidate nomination and development. In: Tsaïoun K, Kate SA, editors. *Admet for medicinal chemists*. Singapore: John Wiley and Sons; 2011. p. 399–415.
- Biovia DS Discovery Studio Modeling Environment. 2015.
- Bohacek RS, McMartin C, Guida WC. The art and practice of structure-based drug design: a molecular modeling perspective. *Med Res Rev*. 1996;16:3–50.
- Burlingham BT, Widlanski TS. An intuitive look at the relationship of K_i and IC_{50} : a more general use for the dixon plot. *J Chem Educ*. 2003;80:214–8.
- Cals JWL, Boumans D, Lardinois RJM, Gonzales R, Hopstaken RM, Butler CC, Dinant GJ. Public beliefs on antibiotics and respiratory tract infections: an internet-based questionnaire study. *Br J Gen Pract*. 2007;57:942–7.
- Caly L, Druce JD, Catton MG, Jans DA, Wagsta KM. The FDA-approved drug Ivermectin inhibits the replication of SARS-CoV-2 in vitro. *Antiviral Res*. 2020;178:104787.
- Carlet J, Collignon P, Goldmann D, Gyssens IC, Harbarth S, Jarlier V, Levy SB, N'Doye B, Pittet D, Richtmann R, Seto WH, van der Meer JW, Voss A. Society's failure to protect a precious resource: antibiotics. *Lancet*. 2011;378:369–71.
- Chan JF, Yuan S, Kok KH, Yuan S, Kai K, Chu H, Yang J, Xing F, Liu J, Yip CC, Poon RW, Tsoi H, Lo SK, Chan K, Poon VK, Chan W, Ip JD, Cai J, Cheng VC, Chen H, Hui CK, Yuen K. A familial cluster of pneumonia associated with the 2019 novel coronavirus indicating person-to-person transmission: a study of a family cluster. *Lancet*. 2020;395:514–23.
- Chang L, Yan Y, Wang L. Coronavirus disease 2019: coronaviruses and blood safety. *Transfus Med Rev*. 2020;34:75–80.
- Chatterjee S, Kumar SH, Yadav N, Mishra V. Click triazole as a linker for drug repurposing against SARs-CoV-2: a greener approach in race to find COVID-19 therapeutic. *Curr Res Green Sustain Chem*. 2021;4:1–12.
- Chen N, Zhou M, Dong X, Qu J, Gong F, Han Y, Qiu Y, Wang J, Liu Y, Wei Y, Xia J, Yu T, Zhang X, Zhang L. Epidemiological and clinical characteristics of 99 cases of 2019 novel coronavirus pneumonia in Wuhan, China: a descriptive study. *Lancet*. 2020;395:507–13.
- Cheng F, Li W, Zhou Y, Shen J, Wu Z, Liu G, Lee PW, Tang Y. admetSAR: a comprehensive source and free tool for assessment of chemical ADMET properties. 2012;52:3099–3105.
- Colson P, Rolain J, Raoult D. Chloroquine for the 2019 novel coronavirus SARS-CoV-2. *Int J Antimicrob Agents*. 2020;55:105923.
- Cortegiani A, Ingoglia G, Ippolito M, Giarratano A, Einav S. A systematic review on the efficacy and safety of chloroquine for the treatment of COVID-19. *J Crit Care*. 2020;57:279–83.
- Daina A, Zoete V. A boiled-egg to predict gastrointestinal absorption and brain penetration of small molecules. *ChemMedChem*. 2016;11:1117–21.
- Falade VA, Adelusi TI, Adedotun IO, Abdul-Hammed M, Lawal TA, Agboluaje SA. In silico investigation of saponins and tannins as potential inhibitors of SARS-CoV-2 main protease (M^{pro}). *Silico Pharmacol*. 2021;9:1–15.
- Ferreira LG, Santos RN, Oliva G, Andricopulo AD. Molecular docking and structure-based drug design strategies. *Molecules*. 2015;20:13384–421.
- Gautret P, Lagier J, Parola P, Hoang VT, Meddeb L, Mailhe M, Doudier B, Courjon J, Giordanengo V, Vieira VE, Tissot Dupont H, Honoré S, Colson P, Chabrière E, La Scola B, Rolain JM, Brouqui P, Raoult D. Hydroxychloroquine and azithromycin as a treatment of COVID-19: results of an open-label non-randomized clinical trial. *Int J Antimicrob Agents*. 2020;56:10549.
- Gopinath S, Kim MV, Rakib T, Wong PW, van Zandt M, Barry NA, Kaisho T, Goodman AL, Iwasaki A. Topical application of aminoglycoside antibiotics enhances host resistance to viral infections in a microbiota-independent manner. *Nat Microbiol*. 2018;3:611–21.
- Gopinath S, Lu P, Iwasaki A, Alerts E. Cutting edge: the use of topical aminoglycosides as an effective pull-in 'prime and pull' vaccine strategy. *J Immunol*. 2020;204:1703–7.
- Guan L, Yang H, Cai Y, Sun L, Di P, Li W, Liu G, Tang Y. ADMET-score-a comprehensive scoring function for evaluation of chemical drug-likeness. *Med Chem Commun*. 2018;10:148–57.
- Hara Y, Hanjo Y. Ofloxacin and levofloxacin (tarivi/cravit). In: Nagaoka S, editor. *Drug discovery in Japan*. Singapore: Springer; 2019. p. 85–110.
- Hopkins AL, Keserü GM, Leeson PD, Rees DC, Reynolds CH. The role of ligand efficiency metrics in drug discovery. *Nat Rev Drug Discov*. 2014;13:105–21.
- Huang S, Zou X. Advances and challenges in protein-ligand docking. *Int J Mol Sci*. 2010;11:3016–34.
- Hughes JP, Rees S, Kalindjian SB, Philpott KL. Principles of early drug discovery. *Br J Pharmacol*. 2011;162:1239–49.
- Kaddoura M, Allbrahim M, Hijazi G, Soudani N, Audi A, Alkalamouni H, Haddad S, Eid A, Zaraket H. COVID-19 therapeutic options under investigation. *Front Pharmacol*. 2020;11:1196.
- Karst SM. The influence of commensal bacteria on infection with enteric viruses. *Nat Rev Microbiol*. 2016;14:197–205.
- Khan AF, Basir R. Sequential intravenous-oral administration of ciprofloxacin vs ceftazidime in serious bacterial respiratory tract infections. *Chest*. 1989;96:528–37.

31. Kumar N, Admane N, Kumari A, Sood D, Grover S, Prajapati VK, Chandra R, Grover A. Cytotoxic T-lymphocyte elicited vaccine against SARS-CoV-2 employing immunoinformatics framework. *Sci Rep*. 2021;11:1–14.
32. Kumar N, Awasthi A, Kumari A, Sood D, Jain P, Singh T, Sharma N, Grover A, Chandra R. Antitussive noscipine and antiviral drug conjugates as arsenal against COVID-19: a comprehensive chemoinformatics analysis. *J Biomol Struct Dyn*. 2020. <https://doi.org/10.1080/07391102.2020.1808072>.
33. Kumar N, Sood D, Chandra R. Vaccine formulation and optimization for human herpes virus-5 through an immunoinformatics framework. *ACS Pharmacol Transl Sci*. 2020;3:1318–29.
34. Kumar N, Sood D, Chandra R. Design and optimization of a subunit vaccine targeting COVID-19 molecular shreds using an immunoinformatics framework. *RSC Adv*. 2020;10:35856–72.
35. Kumar N, Sood D, Gupta A, Kumar Jha N, Jain P, Chandra R. Cytotoxic T-lymphocyte elicited therapeutic vaccine candidate targeting cancer against MAGE-A11 carcinogenic protein. *Biosci Rep*. 2020;40:1–19.
36. Kumar N, Sood D, van der Spek PJ, Sharma HS, Chandra R. Molecular binding mechanism and pharmacology comparative analysis of noscipine for repurposing against SARS-CoV-2 protease. *J Proteome Res*. 2020;19:4678–89.
37. Li Y, Zhang J, Wang N, Li H, Shi Y, Guo G, Liu K, Zeng H, Zou Q. Therapeutic drugs targeting 2019-nCoV main protease by high-throughput screening. *BioRxiv*. <https://doi.org/10.1101/2020.01.28.922922>. 2020.
38. Lipinski CA. Lead, and drug-like compounds: the rule-of-five revolution. *Drug Discov Today*. 2004;1:337–41.
39. Liu X, Zhang B, Jin Z, Yang H, Rao Z. Structure of M^{pro} from COVID-19 virus and discovery of its inhibitors. *Nature*. 2020;582:289–93.
40. López-vallejo F, Caulfield T, Martínez-Mayorga K, Giulianotti MA, Nefzi A, Houghten RA, Medina-Franco JL. Integrating virtual screening and combinatorial chemistry for accelerated drug discovery. *Comb Chem High Throughput Screen*. 2011;14:475–87.
41. Lythgoe MP, Middleton P. Ongoing clinical trials for the management of the COVID-19 pandemic. *Trends Pharmacol Sci*. 2020;41:363–82.
42. Miller A, Reandelar MJ, Fasciglione K, Roumenova V, Li Y, Otazu GH. Correlation between universal BCG vaccination policy on reduced morbidity and mortality for covid-19: an epidemiology study. *MedRxiv*. 2020.
43. Onawole AT, Kolapo TU, Sulaiman KO, Adegoke RO. Structure-based virtual screening of the ebola virus trimeric glycoprotein using consensus scoring. *Comput Biol Chem*. 2018;72:170–80.
44. Onawole AT, Sulaiman KO, Adegoke RO, Kolapo TU. Identification of potential inhibitors against the Zika virus using consensus scoring. *J Mol Graph Mod*. 2017;73:54–61.
45. Oyebamiji AK, Adeleke BB. Theoretical bio-significance evaluation of quinazoline analogues. *Int Res J Pure Appl Chem*. 2019;18:1–8.
46. Retallack H, Di E, Arias C, Knopp KA, Laurie MT, Sandoval-Espinosa C, Mancia Leon WR, Krencik R, Ullian EM, Spatazza J, Pollen AA, Mandel-Brehm C, Nowakowski TJ, Kriegstein AR, DeRisi JL. Zika virus cell tropism in the developing human brain and inhibition by azithromycin. *Proc Natl Acad Sci*. 2016;113:14408–13.
47. Sanguinetti MC, Tristani-firouzi M. hERG potassium channels and cardiac arrhythmia. *Nature*. 2006;440:463–9.
48. Schultes S, De Graaf C, Haaksma EEJ, De Esch IJP, Leurs R, Kramer O. Ligand efficiency as a guide in fragment hit selection and optimization. *Drug Discov Today Technol*. 2010;7:e157–62.
49. Schultes S, Kooistra A, Vischer HF, Nijmeijer S, Haaksma EE, Leurs R, De Esch IJP, de Graaf C. Combinatorial consensus scoring for ligand-based virtual fragment screening: a comparative case study for serotonin 5-HT_{3A}, histamine H₁ and histamine H₄ receptors. *J Chem Inf Model*. 2015;55:1030–44.
50. Singh VK, Kumar N, Chandra R. Structural Insights of Induced pluripotent stem cell regulatory factors Oct4 and its Interaction with Sox2 and Fgf4 Gene. *Adv Biotechnol Biochem*. 2017;119:1–9.
51. Sodhi M, Etminan M. Therapeutic potential for tetracyclines in the treatment of Covid-19. *Pharmacother*. 2020;40:1–2.
52. Stevens E. Lead discovery. In: Jaworski A, editor. *Medicinal chemistry: modern drug discovery process*. Pearson. 2014. 247–272.
53. Sulaiman KO, Kolapo TU, Onawole AT, Islam A, Adegoke RO, Badmus SO. Molecular dynamics and combined docking studies for the identification of zaire ebola virus inhibitors. *J Biomol Struct Dyn*. 2019;37:3029–40.
54. Tanday S. Resisting the use of antibiotics for viral infections. *Lancet Respir Med*. 2016;4:179.
55. Tian W, Chen C, Lei X, Zhao J, Liang J. CASTp 3.0: computed atlas of surface topography of proteins. *Nucl Acids Res*. 2018;46:W363–7.
56. Tong JC. Applications of computer-aided drug design. In: Grover A, editor. *Drug design: principle and applications*. Springer Nature Singapore Pte Ltd; 2017. 1–5.
57. Tran DH, Sugamata R, Hirose T, Suzuki S, Noguchi Y, Sugawara A, Ito F, Yamamoto T, Kawachi S, Akagawa KS, Ōmura S, Sunazuka T, Ito N, Mimaki M, Suzuki K. Azithromycin, a 15-membered macrolide antibiotic, inhibits influenza A (H1N1) pdm09 virus infection by interfering with virus internalization process. *J Antibiot*. 2019;72:759–68.
58. Trott O, Olson AJ. Software news and update autodock vina: improving the speed and accuracy of docking with a new scoring function, efficient optimization, and multithreading. *J Comput Chem*. 2010;31:455–61.
59. Wang JM, Cao R, Zhang L, Yang X, Liu J, Xu M, Shi Z, Hu Z, Zhong W, Xiao G. Remdesivir, and chloroquine effectively inhibit the recently emerged novel coronavirus (2019-nCoV) in vitro. *Cell Res*. 2020;30:269–71.
60. Xue X, Yu H, Yang H, Xue F, Wu Z, Shen W, Li J, Zhou Z, Ding Y, Zhao Q, Zhang XC, Liao M, Bartlam M, Rao Z. Structures of two coronavirus main proteases: implications for substrate binding and antiviral drug design. *J Virol*. 2008;82:2515–27.

Publisher's Note Springer Nature remains neutral with regard to jurisdictional claims in published maps and institutional affiliations.